arXiv:1602.02646v1 [math.NA] 8 Feb 2016

Fast iterative solution of the Bethe-Salpeter eigenvalue problem using low-rank and QTT tensor approximation

Peter Benner* Sergey Dolgov** Venera Khoromskaia◇
Boris N. Khoromskij§

February 9, 2016

Abstract

In this paper, we study and implement the structural iterative eigensolvers for the large-scale eigenvalue problem in the Bethe-Salpeter equation (BSE) based on the reduced basis approach via low-rank factorizations in generating matrices, introduced in the previous paper. The approach reduces numerical costs down to $\mathcal{O}(N_b^2)$ in the size of atomic orbitals basis set, N_b, instead of practically intractable $\mathcal{O}(N_b^6)$ complexity scaling for the direct diagonalization of the BSE matrix. As an alternative to rank approximation of the static screen interaction part of the BSE matrix, we propose to restrict it to a small active sub-block, with a size balancing the storage for rank-structured representations of other matrix blocks. We demonstrate that the enhanced reduced-block approximation exhibits higher precision within the controlled numerical cost, providing as well a distinct two-sided error estimate for the BSE eigenvalues. It is shown that further reduction of the asymptotic computational cost is possible due to ALS-type iteration in block tensor train (TT) format applied to the quantized-TT (QTT) tensor representation of both long eigenvectors and rank-structured matrix blocks. The QTT-rank of these entities possesses almost the same magnitude as the number of occupied orbitals in the molecular systems, N_o, hence the overall asymptotic complexity for solving the BSE problem can be estimated by $\mathcal{O}(\log(N_o)N_o^2)$. We confirm numerically a considerable decrease in computational time for the presented iterative approach applied to various compact and chain-type molecules, while supporting sufficient accuracy.

Key words: Bethe-Salpeter equation, Hartree-Fock calculus, tensor decompositions, quantized-TT format, model reduction, structured eigensolvers, low-rank matrix.
AMS Subject Classification: 65F30, 65F50, 65N35, 65F10

*Max Planck Institute for Dynamics of Complex Technical Systems, Sandtorstr. 1, D-39106 Magdeburg, Germany (benner@mpi-magdeburg.mpg.de)

**University of Bath, The Avenue, Bath, BA2 7AY, United Kingdom (S.Dolgov@bath.ac.uk). S. Dolgov gratefully acknowledges funding from the Engineering and Physical Sciences Research Council (EPSRC) Fellowship EP/M019004/1. This work was mainly conducted when S. Dolgov worked at the Max Planck Institute for Dynamics of Complex Technical Systems, Magdeburg, Germany.

◇Max Planck Institute for Mathematics in the Sciences, Leipzig; Max Planck Institute for Dynamics of Complex Systems, Magdeburg, Germany (vekh@mis.mpg.de).

§Max Planck Institute for Mathematics in the Sciences, Inselstr. 22-26, D-04103 Leipzig, Germany (bokh@mis.mpg.de).

1 Introduction

This paper continues the previous article [5] where the reduced basis approach to the solution of Bethe-Salpeter algebraic eigenvalue problem was introduced, based on the idea of low-rank plus diagonal approximation to the matrix blocks and then solving the small size spectral problem via Galerkin projection onto the reduced basis set.

The Bethe-Salpeter equation (BSE) [42], [15] offers one of the commonly used mathematical models for *ab initio* computation of the absorption spectra for molecules or surfaces of solids, see also [39, 33, 43, 26, 38]. The BSE approach leads to the challenging computational task on the solution of a large eigenvalue problem for fully populated (dense) matrix, that, in general, is non-symmetric. The size of the BSE matrix scales quadratically $\mathcal{O}(N_b^2)$ in a size N_b of the atomic orbitals basis sets, commonly used in *ab initio* electronic structure calculations. Hence, the direct diagonalization of $\mathcal{O}(N_b^6)$-complexity becomes prohibited even for moderate size molecules.

Methods for solving partial eigenvalue problems for matrices with a special structure as in the BSE eigenvalue problem have been intensively studied in the literature. These structures are related to the so called Hamiltonian matrices, exposing a particular block pattern. Papers and books treating Hamiltonian eigenvalue problems include [3, 6, 27, 13], see also the recent survey [8] and the references therein. Special cases of the BSE and other eigenvalue problems related to Hartree-Fock approximations lead to anti-block-diagonal Hamiltonian eigenproblems that can be solved by special techniques based on minimization principles [1, 2]. The algebraic structure of the BSE matrix is not that of a Hamiltonian matrix in the general case, but yields a so called complex J-symmetric matrix. Theory and numerical solution of such eigenvalue problems are discussed in [7, 30, 29, 31, 4], where the particular instance of the BSE matrix is considered in [4]. Other structural eigensolvers tailored for electronic structure calculations are discussed in [40, 41, 9, 32, 28, 45].

Recall that [5] introduces and studies a reduced basis method for the approximate numerical solution of the BSE algebraic eigenvalue problem that is well suited for Krylov subspace type algorithms. This approach is based on model reduction via projection onto a *reduced basis*, which is constructed by using the eigenvectors of a simplified system matrix obeying a diagonal plus low-rank data-sparse structure. The reduced basis method in [5] includes two main computational steps. First, the diagonal plus low-rank approximation to the fully populated blocks in the BSE matrix is calculated, enabling an easier partial eigenvalue solver for a large auxiliary system relying only on matrix-vector multiplications with rank-structured matrices. Second, a small subset of eigenvectors from the auxiliary eigenvalue problem is selected to build the Galerkin projection of the exact BSE system onto this reduced basis set. The adaptive choice of the rank parameters is determined by the ε-thresholding in the matrix factorizations.

Following [5], we use the particular description of the BSE matrix presented in [37]. We build up the BSE system matrix by using the complete output of the Hartree-Fock calculations including rank-structured representation of the two electron integrals (TEI) tensor in the molecular orbital basis precomputed by a grid-based tensor approach [17, 21, 19, 20].

In this paper, we study and implement the structured iterative solvers for the large-scale BSE eigenvalue problem, based on reduced basis approach via low-rank factorizations

in generating matrices [5]. As the alternative to problematic low-rank approximation of the static screen interaction part in the BSE matrix we propose to implement the matrix-vector product with this matrix block using only its restriction to a small sub-block, with a size that balances the complexity of rank-structured representations of the other parts in the system matrix. We show numerically that this enhanced representation considerably improves accuracy of the solution under the controlled numerical cost. The approach reduces the numerical expense of the direct diagonalization down to $\mathcal{O}(N_b^2)$ in the size of the atomic orbitals basis set, N_b.

Several iterative schemes are considered for both the Tamm-Dancoff approximation (TDA) and the full BSE 2×2 block system. The most efficient subspace iteration is based on application of the matrix inverse, which for our matrix formats can be evaluated in a structural form by using the Sherman-Morrison formula. Numerical tests confirm the considerable decrease in computational time for the presented approach, while supporting the sufficient accuracy.

Further reduction of the numerical cost can be achieved by adapting the ALS-type iteration (in particular, DMRG iteration) for computing the eigenvectors in the block-QTT tensor representation [10], where the skeleton vectors of a low-rank part of the matrix are further approximated in the QTT format. Application of the QTT-approximation is motivated by the observation, known from [19], that the generating Cholesky factors in the TEI tensor exhibit the average QTT-ranks proportional only to the number of occupied orbitals in the molecular system, N_o, but they do not depend on the total BSE matrix size, $\mathcal{O}(N_b^2)$. For eigenvectors in the block-QTT format, the QTT ranks are even smaller, typically proportional to the number of the sought eigenvectors, which makes this approach to the BSE very competitive.

The rest of the paper is organized as follows. In Section 2 we recall the reduced basis approach to BSE problem introduced in [5], based on low-rank factorization of the BSE matrix blocks. Next, in Section 3 we describe the enhanced structural representation of the BSE system matrix by the reduced-block approximation to the the static screen interaction sub-matrix. This gainfully supplements the diagonal plus low-rank decompositions of the remaining part of the matrix. The enhanced structured approximation improves the accuracy of the reduced basis method as justified by numerical simulations. Moreover, it provides guaranteed upper and lower error bounds for exact eigenvalues of the BSE problem. Section 4 describes structural iterative solvers for the central part of the spectrum in the simplified auxiliary problem. In this way, the rank-structured approximation to the matrix inverse is constructed based on the Sherman-Morrison formula. Section 5 discusses the benefits of structured iterative solver based on the QTT tensor approximation of vectors and matrices in the framework of ALS-type subspace iterations in block-QTT format. In particular, we present and analyze numerically the algorithm for solving the BSE problem in $\mathcal{O}(\log(N_o)N_o^2)$ complexity scaling, where $N_o \ll N_b$ denotes the number of occupied molecular orbitals. Conclusions underline the main results and outlook directions for forthcoming work.

2 Reduced basis approach to BSE problem revisited

The construction of the BSE matrix includes computations of several auxiliary quantities [37, 5] represented in terms of energy spectrum ε_j, $j = 1, ..., N_b$, and the two-electron integrals (TEI) matrix projected onto the Hartree-Fock molecular orbital basis,

$$V = [v_{ia,jb}] \quad a, b \in \mathcal{I}_v := \{N_o + 1, \ldots, N_b\}, \quad i, j \in \mathcal{I}_o := \{1, \ldots, N_o\},$$

where N_b is the number of GTO basis functions and N_o denotes the number of occupied orbitals (see [19, 5] for more details).

The 2×2-block matrix representation of the Bethe-Salpeter equation reads as the following eigenvalue problem determining the excitation energies ω_n:

$$F \begin{pmatrix} \mathbf{x}_n \\ \mathbf{y}_n \end{pmatrix} \equiv \begin{pmatrix} A & B \\ B^* & A^* \end{pmatrix} \begin{pmatrix} \mathbf{x}_n \\ \mathbf{y}_n \end{pmatrix} = \omega_n \begin{pmatrix} I & 0 \\ 0 & -I \end{pmatrix} \begin{pmatrix} \mathbf{x}_n \\ \mathbf{y}_n \end{pmatrix}, \tag{2.1}$$

where the matrix blocks of size $N_{ov} \times N_{ov}$, with $N_{ov} = N_o(N_b - N_o)$, are defined by

$$A = \boldsymbol{\Delta\varepsilon} + V - \overline{W}, \quad B = V - \widetilde{W}. \tag{2.2}$$

Here, the diagonal part is given by the "energy" matrix

$$\boldsymbol{\Delta\varepsilon} = [\Delta\varepsilon_{ia,jb}] \in \mathbb{R}^{N_{ov} \times N_{ov}} : \quad \Delta\varepsilon_{ia,jb} = (\varepsilon_a - \varepsilon_i)\delta_{ij}\delta_{ab},$$

that can be represented in the Kronecker product form

$$\boldsymbol{\Delta\varepsilon} = I_o \otimes \mathrm{diag}\{\varepsilon_a : a \in \mathcal{I}_v\} - \mathrm{diag}\{\varepsilon_i : i \in \mathcal{I}_o\} \otimes I_v,$$

where I_o and I_v are the identity matrices on respective index sets. Matrices $\widetilde{W}$ and $\overline{W}$ are obtained by certain transformations of the matrix V.

The matrices V and $\widetilde{W}$ are proven to have small ϵ-rank (see [21, 19] and [5], respectively). In particular, there holds

$$V \approx L_V L_V^T, \quad L_V \in \mathbb{R}^{N_{ov} \times R_V}, \quad R_V \leq R_B, \tag{2.3}$$

with the rank estimates $R_V = R_V(\varepsilon) = \mathcal{O}(N_b |\log \varepsilon|)$, and $rank(\widetilde{W}) \leq rank(V)$. It was found that the matrix $\overline{W}$ can be approximated by the low-rank substitute only up to the limited precision ϵ, so that computationally unexpensive approach to get rid of this limitation may be the rank approximation with the constraints $rank(\overline{W}) \leq rank(V)$, see [5].

Matrices in the form (2.1) are called as the J-symmetric, see [4] for implications on the algebraic properties of the BSE matrix. Solutions of equation (2.1) come in pairs: excitation energies ω_n with eigenvectors $(\mathbf{x}_n, \mathbf{y}_n)$, and de-excitation energies $-\omega_n$ with eigenvectors $(\mathbf{x}_n^*, \mathbf{y}_n^*)$. The spectral problem (2.1) can be rewritten in the equivalent form

$$F_1 \begin{pmatrix} \mathbf{x}_n \\ \mathbf{y}_n \end{pmatrix} \equiv \begin{pmatrix} A & B \\ -B^* & -A^* \end{pmatrix} \begin{pmatrix} \mathbf{x}_n \\ \mathbf{y}_n \end{pmatrix} = \omega_n \begin{pmatrix} \mathbf{x}_n \\ \mathbf{y}_n \end{pmatrix}. \tag{2.4}$$

The dimension of the matrix in (2.1) is $2N_oN_v \times 2N_oN_v$, where N_o and N_v denote the number of occupied and virtual orbitals, respectively. In general, N_oN_v is asymptotically of

the order of $\mathcal{O}(N_b^2)$, i.e. the spectral problem (2.1) may become computationally extensive even for moderate size molecules, say for $N_b \approx 100$. Indeed, the direct eigenvalue solver for (2.1) (full diagonalization) appears to be infeasible due to $\mathcal{O}(N_b^6)$ complexity scaling.

The main idea of the *reduced basis approach* introduced in [5] can be described as follows. Instead of solving the partial eigenvalue problem for finding of, say, m_0 eigenpairs satisfying equation (2.4), we first solve the slightly simplified auxiliary spectral problem with a modified matrix F_0. The approximation F_0 is obtained from F_1 by using low-rank approximation of matrices

$$\overline{W} \mapsto \overline{W}_r = L_W L_W^\top, \quad \text{and} \quad \widetilde{W} \mapsto \widetilde{W}_r = Y Z^\top \tag{2.5}$$

in the matrix blocks A and B, respectively, i.e., A and B are replaced by

$$A \mapsto A_0 := \boldsymbol{\Delta\varepsilon} + V - \overline{W}_r \quad \text{and} \quad B \mapsto B_0 := V - \widetilde{W}_r, \tag{2.6}$$

where we assume for simplicity $rank(\overline{W}_r) \le r$ and $rank(\widetilde{W}_r) \le r$. Here we take into account that the matrix V, precomputed by tensor-based Hartree-Fock solver [20], is already represented in the low-rank format (2.3) inherited from the Cholesky decomposition of the TEI matrix B, see [19, 5].

The modified auxiliary problem reads

$$F_0 \begin{pmatrix} \mathbf{u}_n \\ \mathbf{v}_n \end{pmatrix} \equiv \begin{pmatrix} A_0 & B_0 \\ -B_0^* & -A_0^* \end{pmatrix} \begin{pmatrix} \mathbf{u}_n \\ \mathbf{v}_n \end{pmatrix} = \lambda_n \begin{pmatrix} \mathbf{u}_n \\ \mathbf{v}_n \end{pmatrix}. \tag{2.7}$$

This eigenvalue problem is a simplification of (2.4), since now the matrix blocks A_0 and B_0, defined in (2.6), are composed of diagonal and low-rank matrices, see Figures 2.1 and 2.2 illustrating the data sparse structure of these matrix blocks.

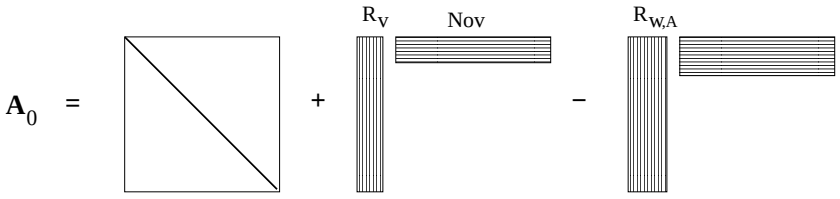

Figure 2.1: Diagonal plus low-rank structure of the matrix A_0.

Having computed the set of eigenpairs $\{(\lambda_n, \psi_n) = (\lambda_n, (\mathbf{u}_n, \mathbf{v}_n)^T)\}$, corresponding to m_0 nearest to zero eigenvalues (middle part of the spectrum) of the modified problem (2.7), we solve the full eigenvalue problem for the reduced matrix (reduced model) obtained by projection of the initial equation onto the problem adapted small basis set $\{\psi_n\}_{n=1}^{m_0}$ of size m_0.

Define a matrix $G_1 = [\psi_1, ..., \psi_{m_0}] \in \mathbb{R}^{2N_{ov} \times m_0}$, whose columns span eigenvectors of the reduced basis, compute the related Galerkin and mass matrices by projection onto the reduced basis specified by the columns in G_1,

$$M_1 = G_1^T F_1 G_1 \in \mathbb{R}^{m_0 \times m_0}, \quad S_1 = G_1^T G_1 \in \mathbb{R}^{m_0 \times m_0},$$

and then solve the reduced generalized eigenvalue problem of small size $m_0 \times m_0$,

$$M_1 \mathbf{q}_n = \gamma_n S_1 \mathbf{q}_n, \quad \mathbf{q}_n \in \mathbb{R}^{m_0}. \tag{2.8}$$

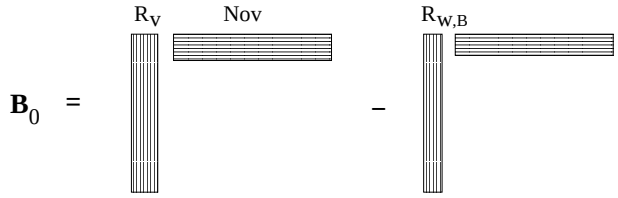

Figure 2.2: Low-rank structure of the matrix B_0.

The portion of m_0 eigenvalues γ_n, is thought to be very close to the lowers excitation energies ω_n, $(n = 1, \ldots, m_0)$ in the initial spectral problem (2.1).

The so-called Tamm-Dancoff approximation (TDA) simplifies the equation (2.4) to a standard Hermitian eigenvalue problem

$$A\mathbf{x}_n = \mu_n \mathbf{x}_n, \quad \mathbf{x}_n \in \mathbb{R}^{N_{ov}} \quad A \in \mathbb{R}^{N_{ov} \times N_{ov}} \tag{2.9}$$

with the factor two smaller matrix size N_{ov}. The reduced basis approach via low-rank approximation can be applied directly to the TDA equation, such that the simplified auxiliary problem reads

$$A_0 \mathbf{u} = \lambda_n \mathbf{u},$$

where we are interested in finding m_0 smallest eigenvalues.

Extensive numerical tests confirm the efficiency of the reduced model approach applied to both TDA and BSE problems for a number of single molecules, as well as to chain type systems [5].

Though the auxiliary eigenvalue equation (2.6), (2.7) is much simpler than (2.4), the computation of dozens of eigenvectors in (2.7) corresponding to the middle part of the spectrum remains to be the challenging numerical task since the traditional algebraic solvers often converge slowly. As a remedy, one can perform matrix-vector operations with the inverse matrix A_0^{-1} or F_0^{-1}. The efficient construction and implementation of the structured matrix inverse A_0^{-1} and F_0^{-1} will be addressed in section 4.

3 Approximating matrix $\overline{W}$ in reduced-block format

Taking into account limitations of the low-rank decomposition to the static screen interaction matrix $\overline{W}$, in what follows, we introduce the alternative way to the data-sparse approximation of this matrix based on its restriction to a smaller-size active sub-matrix.

This approach is motivated by the numerical consideration (observed for all molecular systems considered so far) that eigenvectors corresponding to the central part of the spectrum have dominating components supported by rather small part of the full index set of size $2\,N_{ov}$, see Figure 3.1 for $m_0 = 30$. Indeed, their effective support is compactly located at the first "active" indexes $\{1, ..., N_W\}$ and $\{N_{ov} + 1, ..., N_W\}$ in the respective blocks, where $N_W \ll N_{ov}$.

We define the selected sub-matrix $\overline{W}_b$ in $\overline{W}$, by keeping the balance between the storage size for the active sub-block $\overline{W}_b$ and the storage for the matrix V. Since the storage and numerical complexity of the rank-R_V matrix V is bounded by $2\,R_V\,N_{ov}$, we control the size

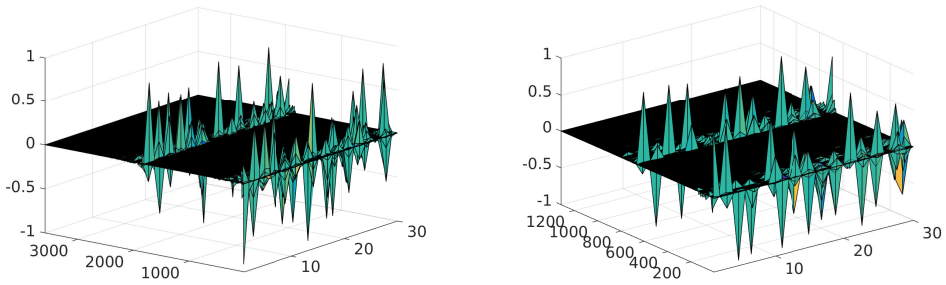

Figure 3.1: Visualizing first m_0 BSE eigenvectors for H_{32} chain and N_2H_4 molecule (right).

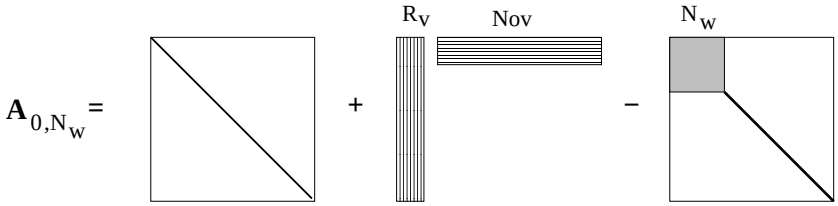

Figure 3.2: Diagonal plus low-rank plus reduced-block structure of the matrix A_{0,N_W}.

of restricted $N_W \times N_W$ block $\overline{W}_b$ by the relation

$$N_W = C_W \sqrt{2\, R_V\, N_{ov}}, \tag{3.1}$$

where the constant $C_W \approx 1$ is close to 1. The approximation error introduced due to the corresponding matrix truncation can be controlled by the choice of constant C_W.

Keeping the diagonal in the matrix $\overline{W}$ unchanged, we define the simplified matrix by $\overline{W} \mapsto W_{N_W} \in \mathbb{R}^{N_{ov} \times N_{ov}}$, where

$$W_{N_W}(i,j) = \begin{cases} \overline{W}(i,j), & i,j \le N_W \quad \text{or} \quad i = j, \quad \text{and} \\ 0 & \text{otherwise.} \end{cases} \tag{3.2}$$

The simplified matrix A_{N_W} is then given by

$$A \mapsto A_{N_W} := \boldsymbol{\Delta\varepsilon} + V - W_{N_W}, \tag{3.3}$$

while the modified block B_0 remains the same as in (2.6). The corresponding structure of the simplified matrix A_{N_W} is illustrated in Figure 3.2.

$C_W \setminus \varepsilon$	0.2	0.1	0.05	0.01
0.8	−0.09; 0.006 (148)	−0.03; 0.04 (213)	−0.008; 0.014 (284)	−0.005; 0.0025 (406)
1.0	−0.1; 0.05 (185)	−0.036; 0.03 (266)	−0.015; 0.0076 (355)	−0.008; 0.0003 (507)
1.2	−0.1; 0.05 (222)	−0.04; 0.02 (320)	−0.017; 0.0038 (426)	$N_W = N_{ov}$

Table 3.1: N_2H_4: Errors $\overline{\lambda}_1 - \omega_1$; $\overline{\gamma}_1 - \omega_1$ (in eV), vs. ε and C_W; N_W is given in brackets.

This construction guaranties that the storage and matrix-vector multiplication complexity for the simplified matrix block A_{N_W} remains of the same order as that for the matrix V characterized by low ϵ-rank.

We modify the auxiliary matrix $F_0 \mapsto \overline{F}_0$ in (2.7) by replacing $A_0 \mapsto A_{N_W}$, which leads to the corrections of the eigenvalues $\lambda_n \mapsto \overline{\lambda}_n$ and eigenvectors $G_1 \mapsto \overline{G}_1 = [\psi_1, ..., \psi_{m_0}] \in \mathbb{R}^{2N_{ov} \times m_0}$ in the simplified problem, $\overline{F}_0 \psi_n = \overline{\lambda}_n \psi_n$. The corresponding eigenvalues $\overline{\gamma}_n$ of the modified reduced system of the type (2.8), specified by the Galerkin matrices

$$\overline{M}_1 = \overline{G}_1^T F_1 \overline{G}_1, \quad \overline{S}_1 = \overline{G}_1^T \overline{G}_1 \in \mathbb{R}^{m_0 \times m_0},$$

solve the eigenvalue problem

$$\overline{M}_1 \mathbf{q}_n = \overline{\gamma}_n \overline{S}_1 \mathbf{q}_n, \quad \mathbf{q}_n \in \mathbb{R}^{m_0}. \tag{3.4}$$

Numerical examples below illustrate the approximation error vs. the rank truncation parameter $\epsilon > 0$ in the reduced basis method characterized by the choice of the constant C_W in the simplified matrix A_{N_W} described in (3.3). Spectral data and errors are given in eV.

$C_W \setminus \varepsilon$	0.2	0.1	0.05	0.01
0.8	−0.23; 0.13 (131)	−0.054; 0.08 (157)	−0.047; 0.06 (168)	−0.006; 0.02 (200)
1.0	−0.28; 0.06 (164)	−0.1; 0.01 (196)	−0.073; 0.015 (210	−0.005; 0.02 (250)
1.2	−0.31; 0.01 (197)	−0.1; 0.01 (236)	−0.074; 0.013 (251)	−0.001; 0.005 (301)

Table 3.2: H_{16} chain: Errors $\overline{\lambda}_1 - \omega_1$; $\overline{\gamma}_1 - \omega_1$ (in eV), vs. ε and C_W; N_W is given in brackets.

Tables 3.1 (N_2H_4 molecule) and Table 3.2 (H_{16} chain) demonstrate the numerical errors $\overline{\lambda}_1 - \omega_1$ and $\overline{\gamma}_1 - \omega_1$ for the minimal BSE eigenvalue ω_1 indicating the two-sided error estimates addressed in Remark 3.1 below.

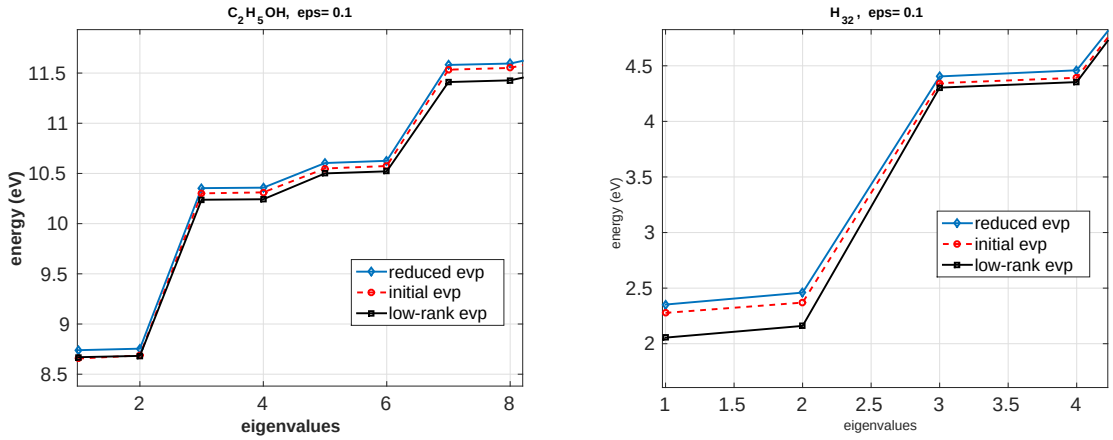

Figure 3.3: Two-sided bounds for the BSE excitation energies for C_2H_5OH and H_{32} chain.

Remark 3.1 *It is worth to note that numerical results indicate the important property observed for all molecular systems tested so far: the close to zero eigenvalues* $\overline{\lambda}_k$ *and* $\overline{\gamma}_k$ *provide the lower and upper bounds for the exact BSE eigenvalues* ω_k*, i.e.*

$$\overline{\lambda}_k \leq \omega_k \leq \overline{\gamma}_k, \quad k = 1, 2, ..., m_0.$$

Figure 3.3 demonstrates the two-sided error estimates declared in Remark 3.1. Here the "black" line represents the eigenvalues for the auxiliary problem of the type (2.7), but with the modified matrix $\overline{F}_0$, while the blue line represents the eigenvalues of the reduced equation (3.4) of the type (2.8) with the Galerkin matrices $\overline{M}_1$ and $\overline{S}_1$.

Figure 3.4 represents examples of upper and lower bounds for the whole sets of m_0 eigenvalues.

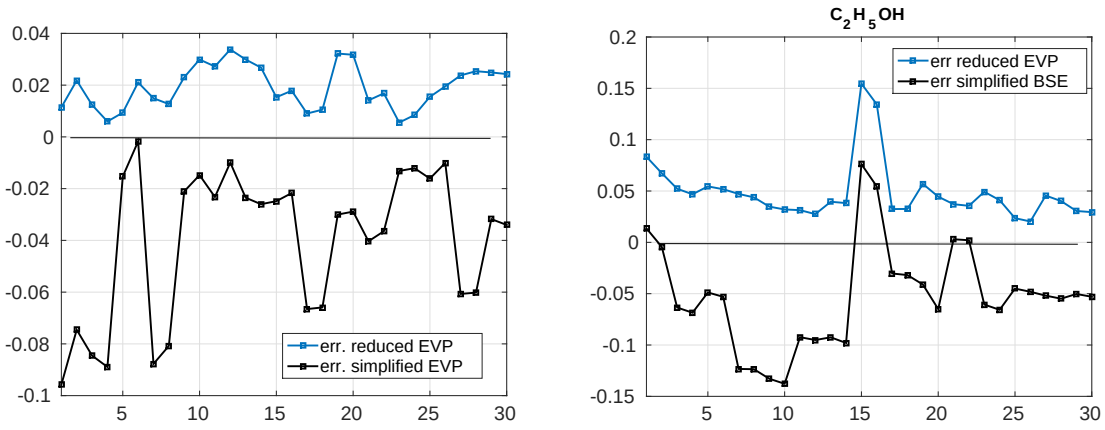

Figure 3.4: The errors (in eV) for simplified and reduced BSE eigenvalues for H_{16} chain and C_2H_5OH molecule (right). Zero level designates the solution of the initial BSE problem.

We conclude that the reduced basis approach based on the modified auxiliary matrix $\overline{F}_0$ via reduced-block anzats (3.3), provides significantly better approximations $\overline{\gamma}_n$ than that for the initial system with the matrix F_0, which is noticeable already for $\overline{\lambda}_n$.

4 Iterative solver for central part of the spectrum

In this section we discuss the construction of iterative solver for partial eigenvalue problem in (2.7) focusing on rank-structured approximation of the matrix inverse A_0^{-1} and F_0^{-1}, further optimization of the sparsity pattern in $\overline{W}$ and on the choice of initial guess by using solutions of the TDA model.

4.1 Inverse iteration for diagonal plus low-rank matrix

Iterative eigenvalue solvers, such as Lancosh or Jacobi-Davidson methods, are quite efficient in approximation of the dominant eigenvalues, but may suffer from slow convergence if applied for computation of the smallest or intermediate eigenvalues. We are interested in both of these scenarios. There are both positive and negative eigenvalues in (2.7), and

we need the few ones with the smallest magnitude. In the TDA model (2.9), we solve a symmetric positive definite problem $A_0\mathbf{u} = \lambda_n\mathbf{u}$, but again the smallest eigenvalues are required.

In both cases, the remedy is to invert the system matrix, so that the eigenvalues of interest become dominant. The Matlab interface to ARPACK (procedure `eigs`) assumes by default that the user-defined function solves a linear system with the matrix instead of multiplying it, when the smallest eigenvalues are requested. In our case, we can implement this efficiently, since the matrix consists of an easily invertible part (diagonal), plus a low-rank correction, and hence we can use the Sherman-Morrison formula.

To shorten the notation, we set up the rank-r decompositions following (2.5), $\overline{W}_r = L_W L_W^\top$, $\widetilde{W}_r = YZ^\top$, and define

$$\begin{aligned} A_0 &= \mathbf{\Delta\varepsilon} + PQ^\top, \qquad P = \begin{bmatrix} L_V & L_W \end{bmatrix}, \quad Q = \begin{bmatrix} L_V & -L_W \end{bmatrix}, \\ B_0 &= \Phi\Psi^\top, \qquad\qquad \Phi = \begin{bmatrix} L_V & Y \end{bmatrix}, \quad \Psi = \begin{bmatrix} L_V & -Z \end{bmatrix}. \end{aligned} \tag{4.1}$$

taking into account (2.3).

Algorithm 1 Precomputation of parts of A_0^{-1} and F_0^{-1}

Require: $\mathbf{\Delta\varepsilon}$ and low-rank factors of V, $\overline{W}_r$, $\widetilde{W}_r$ (2.5).

1: Assemble $P = \begin{bmatrix} L_V & L_W \end{bmatrix}$, $Q = \begin{bmatrix} L_V & -L_W \end{bmatrix}$, $\Phi = \begin{bmatrix} L_V & Y \end{bmatrix}$, $\Psi = \begin{bmatrix} L_V & -Z \end{bmatrix}$.
2: Compute $P_\varepsilon = \mathbf{\Delta\varepsilon}^{-1}P$, $Q_\varepsilon = \mathbf{\Delta\varepsilon}^{-1}Q$.
3: Compute $K = (I + Q^\top P_\varepsilon)^{-1} \in \mathbb{R}^{2r\times 2r}$.
4: Compute $P_{\varepsilon K} = P_\varepsilon K$. {Enough for A_0}
5: Compute $\Phi_\varepsilon = \mathbf{\Delta\varepsilon}^{-1}\Phi$, $\Psi_\varepsilon = \mathbf{\Delta\varepsilon}^{-1}\Psi$.
6: Parts of Q_S: $\Phi_{\varepsilon P} = \Phi_\varepsilon^\top P$, $\Phi_{\varepsilon Q} = Q^\top\Phi_\varepsilon$.
7: Assemble $Q_{S\varepsilon} = \begin{bmatrix} Q_\varepsilon & \Psi_\varepsilon \left(\Phi_{\varepsilon P} K \Phi_{\varepsilon Q} - \Phi^\top\Phi_\varepsilon\right) \end{bmatrix}$, $P_{S\varepsilon} = \begin{bmatrix} P_\varepsilon & \Psi_\varepsilon \end{bmatrix}$.
8: Compute $K_S = (I + \begin{bmatrix} P & \Psi \end{bmatrix}^\top Q_{S\varepsilon})^{-1} \in \mathbb{R}^{4r\times 4r}$
9: Compute $Q_{S\varepsilon K} = Q_{S\varepsilon}K_S$. {For the Schur complement}
10: Compute $\Phi_{AB} = \mathbf{\Delta\varepsilon}^{-1}\Phi - P_{\varepsilon K}\left(Q_\varepsilon^\top\Phi\right)$. {For $A_0^{-1}B_0$}

Algorithm 2 Solution of linear systems with A_0 and F_0

Require: Precomputed matrices $P_{\varepsilon K}, Q_\varepsilon, Q_{S\varepsilon K}, P_{S\varepsilon}, \Phi_{AB}$ from Alg. 1 and $\mathbf{\Delta\varepsilon}, \Phi, \Psi$.

Ensure: $\tilde{\mathbf{z}} = A_0^{-1}\mathbf{u}$ and $\begin{bmatrix} \mathbf{z} \\ \mathbf{y} \end{bmatrix} = F_0^{-1}\begin{bmatrix} \mathbf{u} \\ \mathbf{v} \end{bmatrix}$

1: Apply the TDA inverse as $\tilde{\mathbf{z}} \equiv A_0^{-1}\mathbf{u} = \mathbf{\Delta\varepsilon}^{-1}\mathbf{u} - P_{\varepsilon K}\left(Q_\varepsilon^\top\mathbf{u}\right)$.
2: Compute $\tilde{\mathbf{y}} = \mathbf{v} + \Psi\left(\Phi^\top\tilde{\mathbf{z}}\right)$ (4.4)
3: Apply the Schur complement $\mathbf{y} \equiv S^{-1}\tilde{\mathbf{y}} = -\mathbf{\Delta\varepsilon}^{-1}\tilde{\mathbf{y}} + Q_{S\varepsilon K}\left(P_{S\varepsilon}^\top\tilde{\mathbf{y}}\right)$.
4: Compute $\mathbf{z} = \tilde{\mathbf{z}} - \Phi_{AB}\left(\Psi^\top\mathbf{y}\right)$.

Lemma 4.1 *(Complexity of the diagonal plus low-rank approach). Let the rank parameters in decompositions of V, $\overline{W}$ and $\widetilde{W}$ do not exceed r. Then the rank structured representations*

of inverse matrices A_0^{-1} and F_0^{-1} can be precomputed with the overall cost $\mathcal{O}(N_{ov}r^2)$. The complexity for each inversion $A_0^{-1}\mathbf{u}$ or $F_0^{-1}\mathbf{w}$ is bounded by $\mathcal{O}(N_{ov}r)$.

Proof. We begin with the TDA model (2.9). The Sherman-Morrison formula for A_0 in (4.1) reads

$$A_0^{-1} = \boldsymbol{\Delta\varepsilon}^{-1} - \boldsymbol{\Delta\varepsilon}^{-1}P\left(I + Q^\top\boldsymbol{\Delta\varepsilon}^{-1}P\right)^{-1}Q^\top\boldsymbol{\Delta\varepsilon}^{-1}. \tag{4.2}$$

Here the inner $2r\times 2r$ matrix $K = \left(I + Q^\top\boldsymbol{\Delta\varepsilon}^{-1}P\right)^{-1}$ is small and can be computed explicitly at the expense $\mathcal{O}(r^3+r^2N_{ov})$. Hence matrix-vector product $A_0^{-1}\mathbf{u}_n$ requires multiplication by the diagonal matrix $\boldsymbol{\Delta\varepsilon}^{-1}$ and the low-rank matrix in the second summand. This amounts to the overall cost $\mathcal{O}(N_{ov}r)$.

To invert F_0, we first derive its LU decomposition. One can verify that

$$F_0 = \begin{bmatrix} A_0 & B_0 \\ -B_0^\top & -A_0^\top \end{bmatrix} = \begin{bmatrix} A_0 & 0 \\ -B_0^\top & I \end{bmatrix}\begin{bmatrix} I & A_0^{-1}B_0 \\ 0 & S \end{bmatrix}, \qquad S = -A_0^\top + B_0^\top A_0^{-1}B_0. \tag{4.3}$$

To solve a system $F_0\begin{bmatrix}\mathbf{z}\\ \mathbf{y}\end{bmatrix} = \begin{bmatrix}\mathbf{u}\\ \mathbf{v}\end{bmatrix}$, we need one action of A_0^{-1} and inverse of the Schur complement S^{-1}. Indeed,

$$\begin{aligned} &\tilde{\mathbf{z}} = A_0^{-1}\mathbf{u}, \quad \tilde{\mathbf{y}} = \mathbf{v} + B_0^\top\tilde{\mathbf{z}}, \\ &\mathbf{y} = S^{-1}\tilde{\mathbf{y}}, \quad \mathbf{z} = \tilde{\mathbf{z}} - A_0^{-1}B_0\mathbf{y}. \end{aligned} \tag{4.4}$$

Note that $A_0^{-1}B_0$ is a low-rank matrix and can be precomputed in advance. The action of A_0^{-1} is given by (4.2), so we address now the inversion of the Schur complement.

Plugging (4.2) into S, we obtain

$$S = -\boldsymbol{\Delta\varepsilon} - QP^\top + \Psi\Phi^\top A_0^{-1}\Phi\Psi^\top = -(\boldsymbol{\Delta\varepsilon} + Q_SP_S^\top),$$

where

$$Q_S = \begin{bmatrix} Q & \Psi\left(\Phi^\top\boldsymbol{\Delta\varepsilon}^{-1}PKQ^\top\boldsymbol{\Delta\varepsilon}^{-1}\Phi - \Phi^\top\boldsymbol{\Delta\varepsilon}^{-1}\Phi\right)\end{bmatrix}, \quad P_S = \begin{bmatrix} P & \Psi\end{bmatrix}. \tag{4.5}$$

Therefore,

$$S^{-1} = -\left(\boldsymbol{\Delta\varepsilon}^{-1} - \boldsymbol{\Delta\varepsilon}^{-1}Q_SK_SP_S^\top\boldsymbol{\Delta\varepsilon}^{-1}\right), \quad K_S = \left(I + P_S^\top\boldsymbol{\Delta\varepsilon}^{-1}Q_S\right)^{-1}. \tag{4.6}$$

Keeping intermediate results in these calculations, we can trade off the memory against the CPU time. The computational cost of (4.5) and then (4.6) is again bounded by $\mathcal{O}(r^2N_{ov})$, while the implementation of (4.4) takes $\mathcal{O}(rN_{ov})$ operations. ∎

Lemma 4.1 indicates that for both BSE and TDA models the asymptotic complexity for one iterative step is of the same order. Precomputation of intermediate matrices is described in Algorithm 1, and their use in the structured matrix inversion is shown in Algorithm 2.

Table 4.1 compares CPU times (sec) for full `eig` and rank-structured iteration for TDA problem (2.9) in Matlab implementation. Rank-truncation threshold is $\varepsilon = 0.1$, the number of computed eigenvalues is $m_0 = 30$. Bottom line shows CPU times (sec) of the `eigs` procedure applied with the inverse matrix-vector product $A_0^{-1}\mathbf{u}$ using Algorithm 2 (marked by "inv"). The other lines show results of the corresponding algorithms which used traditional product $A_0\mathbf{u}$ (A_0 in the low-rank form). Notice that the results for Matlab version of LOBPCG by [24] are presented for comparison. We see that the inverse-based method is superior in all tests.

Molecular syst.	H_2O	N_2H_4	C_2H_5OH	H_{32}	$C_2H_5\ NO_2$	H_{48}	$C_3H_7\ NO_2$
TDA size	180^2	657^2	1430^2	1792^2	3000^2	4032^2	4488^2
`eig`(A_0)	0.02	0.5	4.3	9.8	37.6	91	127.4
`lobpcg`(A_0)	0.22	0.6	5.4	2.77	18.2	5.6	34.2
`eigs`(A_0)	0.07	0.29	1.7	0.49	12	2.7	21
`eigs`$(\mathrm{inv}(A_0))$	0.05	0.08	0.17	0.11	0.32	0.34	0.5

Table 4.1: Times (s) for eigensolvers applied to TDA matrix.

Remark 4.2 *Notice that the initial guess for the subspace iteration applied to the full BSE can be constructed, replicating the eigenvectors computed in the TDA model. It provides rather accurate approximation to the exact eigenvectors for the initial BSE system (2.4). In [5] it was shown numerically that the TDA approximation error $|\mu_n - \omega_n|$ of the order of 10^{-2} eV is achieved for compact and extended molecules presented in Table 4.1.*

Table 4.2 compares CPU times (sec) for EIG-solver and rank-structured EIGS-iteration applied to the full BSE problem (2.4).

Molecular syst.	H_2O	N_2H_4	C_2H_5OH	H_{32}	$C_2H_5\ NO_2$	H_{48}	$C_3H_7\ NO_2$
N_o, N_b	5, 41	9 , 82	13, 123	16, 128	20, 170	24, 192	24, 211
BSE matrix size	360^2	1314^2	2860^2	3584^2	6000^2	8064^2	8976^2
`eig`(F_0)	0.08	4.2	33.7	68.1	274	649	903
`eigs`(F_0)	0.13	0.28	0.7	0.77	2.2	2.3	3.9

Table 4.2: Times (s) for the full BSE matrix F_0.

4.2 Inversion of the block-sparse matrices

If W_{N_W} is kept in the block-diagonal form as in (3.3), its inversion remains still easy similar to the case (2.6). Basically, we can use the same Sherman-Morrison scheme from Algorithms 1, and 2. To that end, we aggregate $\mathbf{\Delta\varepsilon}_W = \mathbf{\Delta\varepsilon} - W_{N_W}$, while in the low-rank factors the only $P = Q = L_V$ remains. After that, all calculations in Algorithms 1 and 2 are repeated unchanged, replacing all $\mathbf{\Delta\varepsilon}$ by $\mathbf{\Delta\varepsilon}_W$, where the latter is now a block-diagonal matrix.

The particular modifications for the enhanced algorithm are as follows. Let us split $\mathbf{\Delta\varepsilon} = \mathrm{blockdiag}(\mathbf{\Delta\varepsilon}_1, \mathbf{\Delta\varepsilon}_2)$, where $\mathbf{\Delta\varepsilon}_1$ has the size N_W, and $\mathbf{\Delta\varepsilon}_2 \in \mathbb{R}^{N'_W \times N'_W}$ with $N'_W = N_{ov} - N_W$ represents the remaining values. The same applies to $W_{N_W} = \mathrm{blockdiag}(W_b, \mathrm{diag}(w_2))$, where w_2 contains the elements on the diagonal of W_{N_W} which do not belong to W_b. Then the implementation of the matrix inverse

$$\mathbf{\Delta\varepsilon}_W^{-1} = \mathrm{blockdiag}((\mathbf{\Delta\varepsilon}_1 - W_b)^{-1}, (\mathbf{\Delta\varepsilon}_2 - \mathrm{diag}(w_2))^{-1}) \tag{4.7}$$

requires inversion of an $N_W \times N_W$ dense matrix, and a diagonal matrix of size $N'_W = N_{ov} - N_W$. Since N_W is chosen small, the complexity of this operation is moderate. Now

Molecular syst.	H_2O	N_2H_4	C_2H_5OH	H_{32}	$C_2H_5\ NO_2$	H_{48}	$C_3H_7\ NO_2$
TDA size	180^2	657^2	1430^2	1792^2	3000^2	4032^2	4488^2
TDA: `eigs`(block(A_0))	0.09	0.33	2.8	0.77	16.1	3.0	30
TDA: `eigs`(block-inv(A_0))	0.07	0.09	0.25	0.77	0.54	3.0	1.0
BSE: `eigs`(inv(block(F_0)))	0.21	0.37	1.11	1.10	2.4	2.92	4.6
BSE vs. $\overline{F_0}$: $\lvert\overline{\gamma}_1 - \omega_1\rvert$	0.02	0.03	0.08	0.07	0.05	0.10	0.1

Table 4.3: Block-sparse matrices: times (s) for eigensolvers applied to TDA and BSE systems. Bottom line shows the error (eV) for the case of block-sparse approximation to the diagonal matrix block A_0, $\varepsilon = 0.1$.

all steps requiring multiplication with $\mathbf{\Delta\varepsilon}$ in Algorithm 1–2 can be substituted by (4.7). Numerical complexity of the new inversion scheme is estimated in the next lemma.

Lemma 4.3 *(Complexity of the reduced-block algorithm). Suppose that the rank parameters in the decomposition of V and $\widetilde{W}$ do not exceed r and the block-size N_W is chosen from the equation (3.1).*

Then the rank structured plus reduced-block representations of inverse matrices A_0^{-1} and F_0^{-1} can be set up with the overall cost $\mathcal{O}(N_{ov}^{3/2}r^{3/2}+N_{ov}r^2)$. The complexity of each inversion $A_0^{-1}\mathbf{u}$ or $F_0^{-1}\mathbf{w}$ is bounded by $\mathcal{O}(N_{ov}r)$.

Proof. Inversion of the $N_W \times N_W$ dense block in (4.7) requires $\mathcal{O}(N_W^3)$ operations. Hence, the condition (3.1) ensures that the cost of setting up the matrix (4.7) is bounded by $\mathcal{O}(N_{ov}^{3/2}r^{3/2})$. After that, multiplication of (4.7) by a $N_{ov} \times r$ matrix (e.g. in Line 2 of Alg. 1) requires $\mathcal{O}(N_W^2 r + N'_W r) = \mathcal{O}(N_{ov}(r^2 + r))$ operations. In Alg. 2, multiplication of (4.7) by a vector is performed with the $\mathcal{O}(N_W^2 + N'_W) = \mathcal{O}(N_{ov}r)$ cost. Complexity of the other steps is the same as in Lemma 4.1. ∎

Numerical illustrations for the enhanced data sparsity are presented in Table 4.3.

Notice that the performance of the low-rank and block-sparse solvers is comparable, but the second one provides the better sparsity and higher accuracy in eigenvalues, see §3. Remarkable that the most advanced version of the approach, based on the inverse iteration applied to the diagonal plus low-rank plus reduced-block approximation, outperforms the full eigenvalue solver on several orders of magnitude.

5 Solving BSE spectral problem in the QTT format

5.1 Rank-structured representation of multi-dimensional tensors

A real tensor of order d is defined as an element of finite dimensional Hilbert space $\mathbb{W}_{\mathbf{m}} = \mathbb{R}^{I_1 \times ... \times I_d}$ composed of the d-fold, $M_1 \times ... \times M_d$ real-valued arrays (tensors), where $\mathbf{m} = (M_1, \ldots, M_d)$, and $I_\ell := \{1, ..., M_\ell\}$, $\ell = 1, ..., d$. A tensor $\mathbf{A} \in \mathbb{R}^{I_1 \times ... \times I_d}$ is represented entry-wise by

$$\mathbf{A} = [a(i_1, ..., i_d)] \equiv [a(\mathbf{i})] \equiv [a_{i_1,...,i_d}] \equiv [a_{\mathbf{i}}] \quad \text{with} \quad \mathbf{i} \in \mathcal{I} = I_1 \times ... \times I_d.$$

The Euclidean scalar product, $\langle \cdot, \cdot \rangle : \mathbb{W}_{\mathbf{m}} \times \mathbb{W}_{\mathbf{m}} \to \mathbb{R}$, is defined by

$$\langle \mathbf{A}, \mathbf{B} \rangle := \sum_{\mathbf{i} \in \mathcal{I}} a_{\mathbf{i}} b_{\mathbf{i}}, \quad \mathbf{A}, \mathbf{B} \in \mathbb{W}_{\mathbf{m}}.$$

The storage size for a dth order tensor scales exponentially in d, $\dim(\mathbb{W}_{\mathbf{m}}) = M_1 \cdots M_d$, that causes the so-called "curse of dimensionality". In this section, for ease of presentation we assume $M_\ell = M$ for $\ell = 1, ..., d$.

The efficient low-parametric representations of dth order tensors can be realized by using low-rank separable decompositions (formats). The commonly used canonical and Tucker tensor formats [25] are constructed by linear combination of the simplest separable elements given by rank-1 tensors,

$$\mathbf{U} = \mathbf{u}^{(1)} \otimes ... \otimes \mathbf{u}^{(d)} \in \mathbb{R}^{I_1 \times ... \times I_d}, \quad \mathbf{u}^{(\ell)} \in \mathbb{R}^{M_\ell},$$

with entries $u_{i_1,...i_d} = u^{(1)}_{i_1} \cdots u^{(d)}_{i_d}$, which can be stored by dM numbers.

Tensor-structured numerical methods for PDEs were particularly initiated by employment of the canonical and Tucker tensor formats in grid based "ab initio" electronic structure calculations, namely, for accurate evaluation of the 3D convolution integrals with the Newton kernel, see [20] and references therein. The literature overview on multi-linear algebra and tensor numerical methods for PDEs can be found, for example, in [25, 23, 14, 11, 20].

In this paper we apply the factorized representation of dth order tensors in the tensor train (TT) format [36], which is the particular case of the *matrix product states* (MPS) decomposition [47, 46, 44]. The latter was introduced long since in the physics community and successfully applied in quantum chemistry computations and in spin systems modeling. For a given rank parameter $\mathbf{r} = (r_1, ..., r_{d-1})$, and the respective index sets $J_\ell = \{1, ..., r_\ell\}$ $(\ell = 1, ..., d-1)$, the rank-$\mathbf{r}$ TT format contains all elements $\mathbf{A} = [a(i_1, ..., i_d)] \in \mathbb{W}_{\mathbf{m}}$ which can be represented as the contracted products of 3-tensors over the d-fold product index set $\mathcal{J} := \times_{\ell=1}^{d-1} J_\ell$, such that

$$\mathbf{A} = \sum_{(\alpha_1,...,\alpha_{d-1}) \in \mathcal{J}} \mathbf{a}^{(1)}_{1,\alpha_1} \otimes \mathbf{a}^{(2)}_{\alpha_1,\alpha_2} \otimes \cdots \otimes \mathbf{a}^{(d)}_{\alpha_{d-1},1},$$

or entry-wise

$$a(\mathbf{i}) = \sum_{(\alpha_1,...,\alpha_{d-1})=\mathbf{1}}^{\mathbf{r}} a^{(1)}_{1,\alpha_1}(i_1) a^{(2)}_{\alpha_1,\alpha_2}(i_2) \cdots a^{(d)}_{\alpha_{d-1},1}(i_d) = A^{(1)}(i_1) A^{(2)}(i_2) \cdots A^{(d)}(i_d),$$

with generating vectors $\mathbf{a}^{(\ell)}_{\alpha_{\ell-1},\alpha_\ell} \in \mathbb{R}^{M_\ell}$, and $r_{\ell-1} \times r_\ell$ matrices $A^{(\ell)}(i_\ell) = [a^{(\ell)}_{\alpha_{\ell-1},\alpha_\ell}(i_\ell)]$, $(\ell = 1, ..., d)$ under the convention $r_0 = r_d = 1$. The TT representation reduces the storage cost to $\mathcal{O}(dr^2M)$, $r = \max r_\ell$, $M = \max M_\ell$.

It is often convenient to characterize the TT-rank $\mathbf{r} = (r_1, ..., r_{d-1})$ with a single number. We therefore introduce the notion of the *effective (average) rank* of a TT-tensor $\mathbf{A}$. In the case of equal mode sizes M it is defined as the positive solution of the quadratic equation

$$r_1 + \sum_{k=2}^{d-1} r_{k-1} r_k + r_{d-1} = r + \sum_{k=2}^{d-1} r^2 + r \tag{5.1}$$

and will be denoted by r_{eff} or average QTT rank r.

5.2 Quantized-TT approximation of function related vectors

In the case of large mode size M, the asymptotic storage for a dth order tensor can be reduced to logarithmic scale $\mathcal{O}(d \log M)$ by using quantics-TT (QTT) tensor approximation [22]. In the present paper, we apply this approximation techniques to long N_{ov}-vectors representing the columns of L_V factor and other parts of the BSE matrix, as well as to eigenvectors of the BSE system.

The QTT-type approximation of an M-vector with $M = q^{d'}$, $d' \in \mathbb{N}$, $q = 2, 3, ...$, is defined as the tensor decomposition (approximation) in the TT or canonical format applied to a tensor obtained by the folding (reshaping) of the initial vector to an d'-dimensional $q \times \ldots \times q$ data array. The latter is thought as an element of the multi-dimensional quantized tensor space $\mathbb{Q}_{q,d'} = \bigotimes_{j=1}^{d'} \mathbb{K}^q$, $\mathbb{K} \in \{\mathbb{R}, \mathbb{C}\}$, and d' is the auxiliary dimension (virtual, in contrary to the real space dimension d) parameter that measures the depth of the quantization transform. A vector $\mathbf{x} = [x(i)]_{i \in I} \in \mathbb{W}_M$, is reshaped to its multi-dimensional quantics image in $\mathbb{Q}_{q,d'}$ by q-adic folding,

$$\mathcal{F}_{q,d'} : \mathbf{x} \to \mathbf{Y} = [y(\mathbf{j})] \in \mathbb{Q}_{q,d'}, \quad \mathbf{j} = \{j_1, \ldots, j_{d'}\},$$

with $j_\nu \in \{1, \ldots, q\}$ for $\nu = 1, ..., L$. Here for fixed i, we have $y(\mathbf{j}) := x(i)$, and $j_\nu = j_\nu(i)$ is defined via q-coding, $j_\nu - 1 = C_{-1+\nu}$, such that the coefficients $C_{-1+\nu}$ are found from the q-adic representation of $i - 1$ (binary coding for $q = 2$),

$$i - 1 = C_0 + C_1 q^1 + \cdots + C_{d'-1} q^{d'-1} \equiv \sum_{\nu=1}^{d'} (j_\nu - 1) q^{\nu - 1}.$$

Assuming that for the rank-$\mathbf{r}$ TT approximation of the quantics image $\mathbf{Y}$ there holds $r_k \le r$, $k = 1, \ldots, L$, the complexity of this tensor representation $\mathbf{Y}$ reduces to the logarithmic scale

$$q r^2 \log_q M \ll M.$$

The computational gain of the QTT approximation is justified by the perfect rank decomposition proven in [22] for a wide class of function-related tensors obtained by sampling the corresponding functions over a uniform or properly refined grid. This class of functions includes complex exponentials, trigonometric functions, polynomials and Chebyshev polynomials, wavelet basis functions. We refer to [12, 35, 18, 23] for further results on QTT approximation and their application.

The QTT-type approximation to some $2^{d'} \times 2^{d'}$ matrices was introduced in [34]. The construction and analysis of the QTT representation to the Laplacian related matrices is presented in [16]. The definition of Matrix Product Operator (MPO) is given in §5.4.

In this paper we apply the QTT approximation method to the BSE eigenvalue problem, where matrices and eigenvectors are transformed to the QTT representation and the arising high-dimensional eigenvalue problem is solved by using the block-TT tensor format [10].

5.3 Analysis of the QTT rank parameters for the BSE data

The motivating point for the following considerations in this section was the curious numerical observation discussed in [21, 19]. It was demonstrated that the QTT ranks [22] of

column vectors in the Cholesky factor for the TEI tensor are almost equal to the fundamental structural characteristic of the molecular system, the number of occupied molecular orbitals N_o, i.e. do not depend on the size N_b^2 of the TEI matrix, determined by the number of GTO basis functions N_b. This fact indicates the existence of the tensor-structured QTT representation for the Cholesky factors with the very mild complexity scaling in the matrix size N_b^2.

Here we demonstrate that the very similar property can be observed for the matrices and vectors involved in the BSE spectral problem.

First, we investigate numerically QTT ranks of the long eigenvectors in BSE problem and the canonical QTT ranks in the skeleton vectors of the low-rank matrix factorizations in the case of compact molecules and chains of atoms. Specifically, in numerical tests we found that the QTT-ranks do not depend on the problem size N_{ov} and, hence, on the number of GTO basis functions specifying the size of BSE system, but again depend only on the fundamental physical characteristics of a molecular system, N_o.

Next Table 5.1 illustrates that for the TDA model applied to single molecules and to molecular chains the average QTT ranks, computed for column vectors in L_V factor in (2.3) and for $m_0 = 30$ senior TDA-eigenvectors, are almost equal or even smaller than the number of occupied molecular orbitals, N_o, in the system under consideration. Notice that these results are obtained by compression of each column from L_V or eigenvectors separately. In the next section §5.4, we apply the so-called block-TT format where the meaning of QTT approximation is adapted to the subset of eigenvectors.

Mol. sys.	H_2O	H_{16}	N_2H_4	C_2H_5OH	H_{32}	$C_2H_5\ NO_2$	$C_3H_7\ NO_2$
N_o	5	8	9	13	16	20	24
QTT ranks of L_V	5.4	7	9.1	12.7	14	17.5	21
QTT ranks of e-vectors	5.3	7.6	9.1	12.7	13.6	17.2	20.9
N_{ov}	180	448	657	1430	1792	3000	4488

Table 5.1: Average QTT ranks of column vectors in L_V and m_0 senior eigenvectors in TDA problem.

Table 5.2 demonstrates that the considerable variation of the basis size for fixed molecular systems of H_{12} or H_{24} chains (hence with fixed number N_o) practically does not change the QTT ranks of column vectors in L_V factor in (2.3) (QTT ranks of BSE eigenvectors are almost the same, see Table 5.1).

Figure 5.1 indicates that the behavior of QTT ranks in the column vectors of L_V-factor reproduces the system size N_{ov} in terms of N_o on the logarithmic scale.

It is worth to note that in the case of single molecules the commonly used number of GTO basis sets satisfy the relation $N_b/N_o \geq C_{GTO} \approx 10$ (see examples below), which implies the asymptotic behavior $N_{ov} \approx C_{GTO} N_o^2$. Hence, the QTT rank estimate $r_{QTT} \approx N_o$ obtained above leads to the asymptotic complexity of the QTT-based tensor solver,

$$\mathcal{W}_{BSE} = \mathcal{O}(\log(N_{ov}) r_{QTT}^2) = \mathcal{O}(\log(N_o) N_o^2), \tag{5.2}$$

H_{12}, $N_o = 6$	N_b	36	48	72	84
	size BSE	360^2	504^2	792^2	936^2
	QTT ranks	5.4	6.5	6.6	7.0
H_{24}, $N_o = 12$	N_b	72	96	144	168
	size BSE	1440^2	2016^2	3168^2	3744^2
	QTT ranks	9.5	11.6	11.8	12.7

Table 5.2: Average QTT ranks of column vectors in L_V factor vs. N_o and the BSE-size for Hydrogen chains: illustrates weak dependence on the number of basis functions N_b.

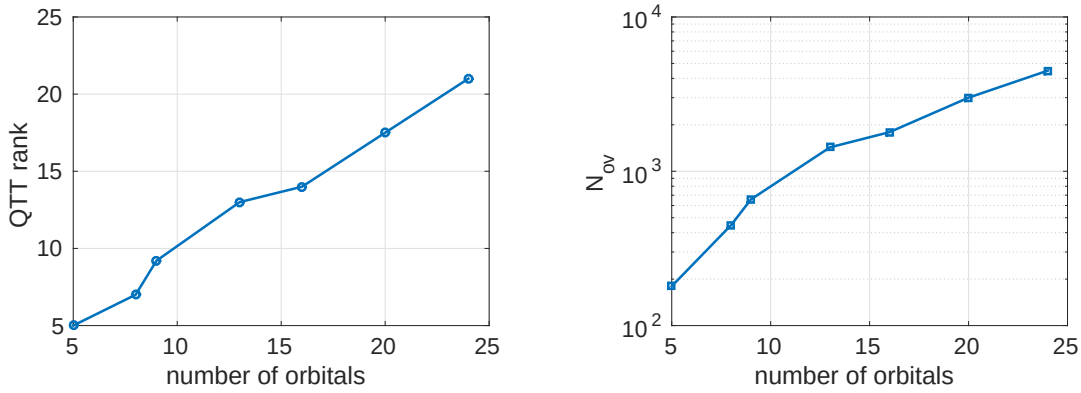

Figure 5.1: QTT ranks (left) and N_{ov} on logarithmic scale (right) vs. the number of orbitals, N_o.

which is asymptotically on the same scale as that for the data-structured algorithms based on full-vector arithmetics (see Section 4). The same observation applies to the chain type molecular systems.

However, the high precision Hartree-Fock calculations may require much larger GTO basis sets so that the constant C_{GTO} may increase considerably. In this situation the QTT-based tensor approach seems to outperform the algorithms in full-vector arithmetics.

Even more important consequence of (5.2) is that the rank behavior $r_{QTT} \approx N_o$ indicates that the QTT tensor-based algorithm has the memory requirements and the algebraic complexity $\mathcal{O}(\log(N_o)N_o^2)$ depending only on the fundamental physical characteristics of the molecular system, the number of occupied molecular orbitals, N_o (but not on the system size N_{ov}^2). Hence, we introduce the *hypothesis*: estimate (5.2) determines the irreducible lower bound on the asymptotic algebraic complexity of the large scale BSE eigenvalue problem.

5.4 Block-TT eigenvalue solver in high-dimensional QTT format

Since the eigenvectors of the TDA problem exhibit moderate QTT ranks, it is tempting to apply the TT eigenvalue solver, such as the DMRG algorithm [47, 44]. As we are always looking for several eigenvectors, we can use the accelerated version [10], where only one TT block is considered at once. The rank adaptivity (as well as fast convergence) comes from the separation of the eigenvalue enumerator from the original index, when we replace the enumerator to the next TT block.

This algorithm can be adapted to the input data we have in the Bethe-Salpeter problem.

In the general setting, given an eigenvalue problem $AU = U\Lambda$, the method assumes that the matrix is given in the matrix TT (also called as Matrix Product Operator) format

$$A(\mathbf{i},\mathbf{j}) = \mathbf{A}^{(1)}(i_1,j_1)\mathbf{A}^{(2)}(i_2,j_2)\cdots\mathbf{A}^{(d')}(i_{d'},j_{d'}), \tag{5.3}$$

where $\mathbf{i}$ and $\mathbf{j}$ are multi-indices comprised from $i_1,\ldots,i_{d'}$ and $j_1,\ldots,j_{d'}$, respectively. Each term $\mathbf{A}^{(l)}(i_l,j_l)$ in the right-hand side is a $r_{l-1}\times r_l$ matrix, similarly to the "vector" TT format, but parametrized by two original indices i_l, j_l, $1 \le i_l, j_l \le q_\ell$. Here we use the general notation d' for the dimension parameter used in the description of QTT format in §5.2. The mode size M_ℓ in the general definition of TT format is substituted by q_ℓ for the QTT tensors.

A slight generalization of the QTT format introduced in Section 5.2 involves different *prime* dimensions of a tensor, instead of the same value q. Given initial dimensions N_o and N_v, we decompose these numbers into smallest nontrivial prime factors, say,

$$N_o = q_1\cdots q_o, \quad N_v = q_{o+1}\cdots q_{d'},$$

such that the total problem size $N_{ov} = q_1\cdots q_{d'}$ yields the corresponding index factorization, allowing the TT format (5.3). If N_o and N_v are powers of 2, we end up with the classical QTT format with $2\times\cdots\times 2$-tensors. But in a more general case, any other small factors (like $3, 5, 7$, and so on) are possible.

The eigenvectors are sought in the block QTT format

$$U_m(\mathbf{i}) = \mathbf{U}^{(1)}(i_1)\cdots\mathbf{U}^{(\ell-1)}(i_{\ell-1})\hat{\mathbf{U}}^{(\ell)}(i_\ell,m)\mathbf{U}^{(\ell+1)}(i_{\ell+1})\cdots\mathbf{U}^{(d')}(i_{d'}), \tag{5.4}$$

where $\hat{\mathbf{U}}^{(\ell)}$ is a special TT block, containing the eigenvector enumerator $m = 1,\ldots,m_0$. Using the SVD, one can decompose $\hat{\mathbf{U}}^{(\ell)}$ and move m to a neighboring block [10]. In this paper, we only need to know that the DMRG technique is a Galerkin projection method: the remaining blocks $\mathbf{U}^{(p)}$, $p\neq\ell$, constitute the *frame* matrix $U_{\neq\ell}\in\mathbb{R}^{N_{ov}\times r_{\ell-1}q_\ell r_\ell}$,

$$U_{\neq\ell}(\mathbf{i},\alpha_{\ell-1}j_\ell\alpha_\ell) = \mathbf{U}^{(1)}(i_1)\cdots\mathbf{U}^{(\ell-1)}_{:,\alpha_{\ell-1}}(i_{\ell-1})\delta_{i_\ell,j_\ell}\mathbf{U}^{(\ell+1)}_{\alpha_\ell,:}(i_{\ell+1})\cdots\mathbf{U}^{(d')}(i_{d'}),$$

such that the *local* problem reads

$$\left(U_{\neq\ell}^\top A U_{\neq\ell}\right)\hat{u}^{(\ell)} = \hat{u}^{(\ell)}\Lambda, \qquad \hat{u}^{(\ell)}\in\mathbb{R}^{r_{\ell-1}q_\ell r_\ell\times m_0}, \tag{5.5}$$

where the diagonal Λ contains the Ritz values, approximating the eigenvalues of the original problem. After solving this problem, the block $\hat{\mathbf{U}}^{(\ell)}$ is populated with the elements of $\hat{u}^{(\ell)}$, and the process continues for the next block.

Numerical experiments show that $\boldsymbol{\Delta\varepsilon}$ and $\overline{W}$ are well compressible in the matrix QTT format (5.3). However, this is not the case for V. We utilize the fact that V can be well approximated by a low-rank matrix, $V = L_V L_V^\top$. The factor L_V has the same conceptual meaning as the eigenvectors: it is a horizontal stack of R vectors of length N. Hence we can use the block TT format (5.4) for L_V (replacing U by L_V). It is even easier since we do not need to move the enumerator m, but can fix it in the last TT block. In each DMRG step, the projected matrix (5.5) is constructed as

$$U_{\neq\ell}^\top A U_{\neq\ell} = U_{\neq\ell}^\top\boldsymbol{\Delta\varepsilon}U_{\neq\ell} + \left(U_{\neq\ell}^\top L_V\right)\left(U_{\neq\ell}^\top L_V\right)^\top - U_{\neq\ell}^\top\overline{W}U_{\neq\ell},$$

where each product is implemented in a fast way, using the TT formats of $U_{\neq\ell}$, $\boldsymbol{\Delta\varepsilon}$, L_V and $\overline{W}$.

H_{12}, $N_o = 6$, 1 DMRG iter	N_b	36	48	72	84
	CPU time	0.019	0.02	0.034	0.04
	av. QTT rank	19.0	20.2	22.0	22.6
	$\frac{\texttt{mem}(\text{QTT})}{N_{ov}m_0}$	1.07	1.00	0.94	0.92
	$\frac{\|\mu_{qtt}-\mu_\star\|}{\|\mu_\star\|}$	2.86e-2	1.22e-2	4.60e-3	8.41e-3
H_{12}, $N_o = 6$, 2 DMRG iters	CPU time	0.02	0.04	0.06	0.08
	av. QTT rank	9.7	14.5	14.7	13.9
	$\frac{\texttt{mem}(\text{QTT})}{N_{ov}m_0}$	0.25	0.35	0.23	0.18
	$\frac{\|\mu_{qtt}-\mu_\star\|}{\|\mu_\star\|}$	3.29e-3	6.36e-3	5.84e-3	7.03e-3
H_{24}, $N_o = 12$ 1 DMRG iter	N_b	72	96	144	168
	CPU time	0.10	0.17	0.09	0.12
	av. QTT rank	21.8	22.5	23.5	23.7
	$\frac{\texttt{mem}(\text{QTT})}{N_{ov}m_0}$	0.42	0.36	0.66	0.74
	$\frac{\|\mu_{qtt}-\mu_\star\|}{\|\mu_\star\|}$	1.95e-1	1.10e-1	6.8e-2	5.8e-2
H_{24}, $N_o = 12$ 2 DMRG iters	CPU time	0.06	0.1	0.23	0.21
	av. QTT rank	13.5	19.8	17.7	17.8
	$\frac{\texttt{mem}(\text{QTT})}{N_{ov}m_0}$	0.14	0.20	0.3	0.3
	$\frac{\|\mu_{qtt}-\mu_\star\|}{\|\mu_\star\|}$	6.43e-3	9.50e-3	8.69e-3	8.97e-3

Table 5.3: DMRG iteration in block-QTT format for TDA model with $m_0 = 30$ sought eigenvalues and all low-rank approximation thresholds 0.1. $\mu_\star$ is computed for the exact TDA matrix (2.9).

Remark 5.1 *Note that here $\overline{W}$ is the original matrix from* (2.2)*, compressed in the matrix QTT format* (5.3)*. No additional low-rank or block-diagonal constraints are imposed. Therefore the results of the DMRG method in this section should be compared directly to the result of the exact eigenvalue solver.*

The reduced eigenvalue problem (5.5) has the size $r_{\ell-1}q_\ell r_\ell$ and can be solved using the full `eig`. The only explicitly iterative part is a sweep over different TT blocks in the alternating fashion. By "iteration", we mean the sequential sweep from the first to the d'-th TT block, or the other way around.

The numerical results are presented in Table 5.3: CPU time (sec.), average QTT rank, memory ratio (the storage of the QTT format over the total number of elements in the full representation) and the relative error of the eigenvalues. We use the tolerance 10^{-6} to compress $\mathbf{\Delta\varepsilon}$ into the matrix TT format[1], but for all other approximations, including the factorization $V = L_V L_V^\top$, the tolerance is set to $\varepsilon = 0.1$. We notice that one DMRG iteration gives insufficient accuracy of the solution, but the second iteration delivers a relative error below the theoretical estimate ε^2. The CPU time is comparable or smaller than the time of the best Sherman-Morrison inversion methods in the previous section, as demonstrated in

[1]This accuracy is necessary, since $\mathbf{\Delta\varepsilon}$ is the dominant part of the matrix. Fortunately, the TT ranks of $\mathbf{\Delta\varepsilon}$ are below 10 even for such accuracy, whereas the ranks of L_V and $\overline{W}$ may exceed a hundred.

Table 5.4 (cf. Table 4.3). Recall that the row "absolute error" in Table 5.4 represents the quantity $\|\mu_{qtt} - \mu_\star\| = (\sum_{m=1}^{m_0}(\mu_{qtt,m} - \mu_{\star,m})^2)^{1/2}$ characterizing the total absolute error in the first m_0 eigenvalues calculated in the Euclidean norm.

Molecular syst.	C_2H_5OH	H_{32}	$C_2H_5\ NO_2$	H_{48}	$C_3H_7\ NO_2$
TDA size	1430^2	1792^2	3000^2	4032^2	4488^2
time QTT eig	0.14	0.23	0.32	0.28	0.63
abs. error (eV)	0.08	0.19	0.17	0.14	0.00034

Table 5.4: Time (s) and absolute error (eV) for QTT-DMRG eigensolvers for TDA matrix.

The QTT format provides also a considerable reduction of memory needed to store eigenvectors.

6 Conclusions

This paper presents efficient iterative solution of the Bethe-Salpeter large-scale eigenvalue problem using the reduced basis approach via low-rank factorizations introduced in [5].

For the static screen interaction part of the BSE submatrix, which was problematic for the low-rank representation in [5], we have found a beneficial substitution by a small sub-block, which reduces the approximation error by the order of magnitude. Moreover, it provides the two-sided error bounds for the exact BSE excitation energies in the case of compact and chain-type molecular systems.

We show that the structured inverse iterations (by using matrix inverse) provide fast convergence for calculation of the required central part of the BSE spectrum. For both BSE and TDA models, the inverse matrix can be represented in the same diagonal plus low-rank plus reduced-block format by using the Sherman-Morrison scheme. The estimates on the complexity of algorithms for diagonal plus low-rank plus reduced-block inverse iterations are presented in Lemmas 4.1 and 4.3.

Solution of the BSE spectral problem in the QTT format is disscussed in detail. The QTT tensor transform of the initial BSE system to the higher dimensional setting allows to construct a structural solver of the complexity $\mathcal{O}(\log(N_o)N_o^2)$, see (5.2). This complexity it is determined by only the number of occupied orbitals, N_o, in the molecular system (i.e. on physical characteristics of the molecule), but it is almost independent of the system size determined by the number of atomic orbitals basis functions, N_b. In numerical tests we observe dramatical reduction of solution time. For example, TDA calculations in QTT format for C_2H_5OH molecule with matrix size 1430^2 take 0.14 sec, while for $C_3H_7NO_2$ (Alanine amino acid) with TDA matrix size 4488^2 CPU time increases only to 0.63 sec.

The results are confirmed by a number of numerical tests conducted through out the paper for various moderate size molecules and molecular chains. Note that the solution of the eigenvalue problem with the rank-structured representation of the BSE matrix reduces calculation times for large enough molecules at least by two orders of magnitude, see, for example, Table 4.2, where for Alanine amino-acid, with the matrix size 8976^2, direct calculation takes 903 s, while the low-rank iteration takes 4 s. Further reduction of complexity is

achieved when using the DMRG-type iteration in the block-QTT tensor format, see Tables 5.3, 5.4.

Several directions for future research work on the rank-structured reduced basis method for computation of excitation energies of molecules and solids will be considered. Particularly, this includes comprehending the considered BSE model by some additional correction terms, developments of the new data-sparse matrix structures, and further applications of algorithms to large and lattice-structured molecular systems.

References

[1] Z. Bai and R.-C. Li. Minimization principle for linear response eigenvalue problem, I: Theory. *SIAM J. Matrix Anal. Appl.*, 33(4):10751100, 2012.

[2] Z. Bai and R.-C. Li. Minimization principle for linear response eigenvalue problem, II: Computation. *SIAM J. Matrix Anal. Appl.*, 34(2):392–416, 2013.

[3] P. Benner and H. Faßbender. An implicitly restarted symplectic Lanczos method for the Hamiltonian eigenvalue problem. *Linear Algebra Appl.*, 263:75–111, 1997.

[4] P. Benner, H. Faßbender, and C. Yang. Some remarks on the complex J-symmetric eigenproblem. Preprint MPIMD/15-12, Max Planck Institute Magdeburg, July 2015.

[5] P. Benner, V. Khoromskaia, and B. N. Khoromskij. A reduced basis approach for calculation of the Bethe-Salpeter excitation energies using low-rank tensor factorizations. *Molecular Physics, DOI: 10.1080/00268976.2016.1149241*, (arXiv:1505.02696v1, 2015), 2016.

[6] P. Benner, V. Mehrmann, and H. Xu. A numerically stable, structure preserving method for computing the eigenvalues of real Hamiltonian or symplectic pencils. *Numerische Mathematik*, 78(3):329–358, 1998.

[7] A. Bunse-Gerstner, R. Byers, and V. Mehrmann. A chart of numerical methods for structured eigenvalue problems. *SIAM J. Matrix Anal. Appl.*, (13):419–453, 1992.

[8] A. Bunse-Gerstner and H. Faßbender. Breaking Van Loan's curse: A quest for structure-preserving algorithms for dense structured eigenvalue problems. In P. Benner, M. Bollhöfer, D. Kressner, C. Mehl, and T. Stykel, editors, *Numerical Algebra, Matrix Theory, Differential-Algebraic Equations and Control Theory*, pages 3–23. Springer International Publishing, 2015.

[9] J. Deslippe, G. Samsonidze, D. A. Strubbe, M. Jain, M. L. Cohen, and S. Louie. BerkeleyGW: A massively parallel computer package for the calculation of the quasi-particle and optical properties of materials and nanostructures. *Comp. Phys. Communications*, 183:1269–1289, 2012.

[10] S. Dolgov, B. Khoromskij, D. Savostyanov, and I. Oseledets. Computation of extreme eigenvalues in higher dimensions using block tensor train formats. *Comp. Phys. Communications*, 185(4):1207–1216, 2014.

[11] S. V. Dolgov. *Tensor product methods in numerical simulation of high-dimensional dynamical problems.* PhD thesis, University of Leipzig, 2014.

[12] S. V. Dolgov, B. N. Khoromskij, and I. V. Oseledets. Fast solution of multi-dimensional parabolic problems in the tensor train/quantized tensor train–format with initial application to the Fokker-Planck equation. *SIAM J. Sci. Comput.*, 34(6):A3016–A3038, 2012.

[13] H. Faßbender and D. Kressner. Structured eigenvalue problem. *GAMM Mitteilungen*, 29(2):297–318, 2006.

[14] L. Grasedyck, D. Kressner, and C. Tobler. A literature survey of low-rank tensor approximation techniques. *arXiv:1302.7121v1*, 2013.

[15] L. Hedin. New method for calculating the one-particle Green's function with application to the electron-gas problem. *Phys. Rev.*, 139:A796, 1965.

[16] V. A. Kazeev and B. N. Khoromskij. Low-rank explicit QTT representation of the Laplace operator and its inverse. *SIAM J. Matrix Anal. Appl.*, 33(3):742–758, 2012.

[17] V. Khoromskaia. Black box Hartree-Fock solver by the tensor numerical methods. *Comp. Methods in Applied Math.*, 14:89–111, 2014.

[18] V. Khoromskaia and B. N. Khoromskij. Grid-based lattice summation of electrostatic potentials by assembled rank-structured tensor approximation. *Comp. Phys. Communications*, 185(12):3162–3174, 2014.

[19] V. Khoromskaia and B. N. Khoromskij. Møller-Plesset (MP2) energy correction using tensor factorizations of the grid-based two-electron integrals. *Comp. Phys. Communications*, 185(1):2–10, 2014.

[20] V. Khoromskaia and B. N. Khoromskij. Tensor numerical methods in quantum chemistry: from Hartree-Fock to excitation energies. *Phys. Chem. Chem. Phys.*, 17:31491 – 31509, 2015.

[21] V. Khoromskaia, B. N. Khoromskij, and R. Schneider. Tensor-structured calculation of two-electron integrals in a general basis. *SIAM J. Sci. Comput.*, 35(2):A987–A1010, 2013.

[22] B. N. Khoromskij. $O(d \log N)$-quantics approximation of N-d tensors in high-dimensional numerical modeling. *J. Constr. Approx.*, 34(2):257–289, 2011.

[23] B. N. Khoromskij. Tensor Numerical Methods for Multidimensional PDEs: Basic Theory and Initial Applications. *ESAIM: Proceedings and Surveys, N. Champagnat, T. Leliévre, A. Nouy, eds*, 48:1–28, January 2015.

[24] A. V. Knyazev. Toward the optimal preconditioned eigensolver: Locally optimal block preconditioned conjugate gradient method. *SIAM Journal on Scientific Computing*, 23(2):517–541, 2001.

[25] T. Kolda and B. W. Bader. Tensor decompositions and applications. *SIAM Review*, 51(3):455–500, 2009.

[26] S. Körbel, P. Boulanger, I. Duchemin, X. Blase, M. AL Marques, and S. Botti. Benchmark many-body GW and Bethe-Salpeter calculations for small transition metal molecules. *Journal of Chemical Theory and Computation*, 10(9):3934–3943, 2014.

[27] D. Kressner. *Numerical Methods for General and Structured Eigenvalue Problems*, volume 46 of *Lecture Notes in Computational Science and Engineering*. Springer, Berlin/Heidelberg, 2005.

[28] L. Lin, Y. Saad, and C. Yang. Approximating spectral densities of large matrices. *ArXiv:1308.5467.v2.*, 2015.

[29] D. Mackey, N. Mackey, C. Mehl, and V. Mehrmann. Structured polynomial eigenvalue problems: good vibrations from good linearizations. *SIAM J. Matrix Anal. Appl.*, 28(4):1029–1051, 2006.

[30] D. Mackey, N. Mackey, and F. Tisseur. Structured tools for structured matrices. *Electronic Journal of Linear Algebra (ELA)*, 10:106–145, 2003.

[31] C. Mehl. On asymptotic convergence of nonsymmetric Jacobi algorithms. *SIAM J. Matrix Anal. Appl.*, 30:291–311, 2008.

[32] E. Napoli, E. Polizzi, and Y. Y. Saad. Efficient estimation of eigenvalue counts in an interval. *arXiv:1308.4275v2*, 2014.

[33] G. Onida, L. Reining, and A. Rubio. Electronic excitations: density-functional versus many-body Green's-function approaches. *Rev. of Modern Physics*, 74:601–659, 2002.

[34] I. V. Oseledets. Approximation of $2^d \times 2^d$ matrices using tensor decomposition. *SIAM J. Matrix Anal. Appl.*, 31(4):2130–2145, 2010.

[35] I. V. Oseledets. Constructive representation of functions in low-rank tensor formats. *Constr. Appr.*, 37(1):1–18, 2013.

[36] I. V. Oseledets and E. E. Tyrtyshnikov. Breaking the curse of dimensionality, or how to use SVD in many dimensions. *SIAM J. Sci. Comput.*, 31(5):3744–3759, 2009.

[37] E. Rebolini, J. Toulouse, and A. Savin. Electronic excitation energies of molecular systems from the Bethe-Salpeter equation: Example of H_2 molecule. *In: Concepts and Methods in Modern Theoretical Chemistry (S. Ghosh and P. Chattaraj eds), vol 1: Electronic Structure and Reactivity*, page 367, 2013.

[38] E. Rebolini, J. Toulouse, A. M. Teale, T. Helgaker, and A. Savin. Calculating excitation energies by extrapolation along adiabatic connections. *Phys. Rev. A*, 91:032519, 2015.

[39] L. Reining, V. Olevano, A. Rubio, and G. Onida. Excitonic effects in solids described by time-dependent density functional theory. *Phys. Rev. Lett.*, 88:066404, 2002.

[40] D. Rocca, R. Gebauer, Y. Saad, and S. Baroni. Turbo charging time-dependent density-functional theory with Lanczos chains. *J. Chem. Phys.*, 128:154104, 2008.

[41] D. Rocca, D. Lu, and G. Galli. *Ab Initio* calculations of optical absorption spectra: Solution of the Bethe-Salpeter equation within density matrix perturbation theory. *J. Chem. Phys.*, 133:164109 1–10, 2010.

[42] E. E. Salpeter and H. A. Bethe. A relativistic equation for bound-state problems. *Phys. Review*, 82(2):309–310, 1951.

[43] W. G. Schmidt, S. Glutsch, P. H. Hahn, and F. Bechstedt. Efficient $O(N^2)$ method to solve the Bethe-Salpeter equation. *Phys. Review B*, 67:085307, 2003.

[44] U. Schollwöck. The density-matrix renormalization group in the age of matrix product states. *Ann.Phys.*, 51(326):96–192, 2011.

[45] M. Shao, F. H. da Jornada, C. Yang, J. Deslippe, and S. Louie. Structure preserving parallel algorithms for solving the Bethe-Salpeter eigenvalue problem. *Linear Algebra and its Applications*, 488:148–167, 2016.

[46] G. Vidal. Efficient classical simulation of slightly entangled quantum computations. *Phys. Rev. Lett.*, 91(14), 2003.

[47] S. R. White. Density-matrix algorithms for quantum renormalization groups. *Phys. Rev. B*, 48(14):10345–10356, 1993.